British Journal of Pharmacology (2006) 149, 880–887
 0007–1188/06 $30.00
www.brjpharmacol.org

# RESEARCH PAPER

# Characterization of a selective and potent antagonist of human $P2X_7$ receptors, AZ11645373

L Stokes[1], L-H Jiang[1], L Alcaraz[2], J Bent[3], K Bowers[3], M Fagura[3], M Furber[2], M Mortimore[3], M Lawson[3], J Theaker[3], C Laurent[3], M Braddock[3] and A Surprenant[1]

[1]*Department of Biomedical Science, University of Sheffield, Sheffield, UK;* [2]*Department of Medicinal Chemistry, AstraZeneca R & D Charnwood, Loughborough, UK and* [3]*Department of Discovery Biosciences, AstraZeneca R & D Charnwood, Loughborough, UK*

**Background and purpose:** The ATP-gated $P2X_7$ receptor has been shown to play a role in several inflammatory processes, making it an attractive target for anti-inflammatory drug discovery. We have recently identified a novel set of cyclic imide compounds that inhibited $P2X_7$ receptor-mediated dye uptake in human macrophage THP-1 cells. In this study the actions and selectivity of one of these compounds, AZ11645373, were characterized.
**Experimental approach:** We measured membrane currents, calcium influx, and YOPRO-1 uptake from HEK cells expressing individual P2X receptors, and YOPRO1 uptake and interleukin-1β release from THP-1 cells in response to ATP and the ATP analogue benzoylbenzoyl ATP (BzATP).
**Key results:** AZ11645373 up to 10 μM, had no agonist or antagonist actions on membrane currents due to P2X receptor activation at human $P2X_1$, rat $P2X_2$, human $P2X_3$, rat $P2X_{2/3}$, human $P2X_4$, or human $P2X_5$ receptors expressed in HEK cells. AZ11645373 inhibited human $P2X_7$ receptor responses in HEK cells in a non-surmountable manner with $K_B$ values ranging from 5 - 20 nM, with mean values not significantly different between assays. $K_B$ values were not altered by removing extracellular calcium and magnesium. ATP-evoked IL-1β release from lipopolysaccharide-activated THP-1 cells was inhibited by AZ11645373, $IC_{50} = 90$ nM. AZ11645373 was $>$ 500-fold less effective at inhibiting rat $P2X_7$ receptor-mediated currents with less than 50% inhibition occurring at 10 μM.
**Conclusions and implications:** AZ11645373 is a highly selective and potent antagonist at human but not rat $P2X_7$ receptors and will have much practical value in studies of human cells.
*British Journal of Pharmacology* (2006) **149,** 880–887. doi:10.1038/sj.bjp.0706933; published online 9 October 2006

**Keywords:** cyclic imides; purine receptors; heterologous expression; receptor antagonist

**Abbreviations:** ATP, adenosine 5′-triphosphate; BzATP, 2′-3′-*O*-(4-benzoylbenzoyl) adenosine 5′-triphosphate; HEK293, human embryonic kidney cell line; $IC_{50}$, half-maximal antagonist concentration; IL-1$\beta$, interleukin-1$\beta$; $K_B$, antagonist affinity constant; LPS, lipopolysaccharide

## Introduction

Adenosine 5′-triphosphate (ATP)-gated P2X receptors (P2XRs) comprise a family of seven gene products which encode plasma membrane ion channels selective for cations including calcium (North, 2002; Vial *et al*., 2004). They are differentially expressed throughout autonomic, sensory and central neurones as well as in visceral smooth muscle, immune cells and epithelia (North, 2002; Burnstock and Knight, 2004). Because externally applied ATP is a well-known nociceptive agent and because it is released from damaged or stressed cells at areas of inflammation and injury, P2XRs have been the subject of many investigations into their potential roles in acute and/or chronic pain sensation. Currently, four of these receptors have been implicated in distinct processes underlying chronic inflammatory and neuropathic pain; these are homomeric $P2X_3$Rs, heteromeric $P2X_{2/3}$Rs, $P2X_4$Rs and $P2X_7$Rs (Jarvis, 2003; North 2004; Liu and Salter, 2005; Tsuda *et al*., 2005).

In the case of $P2X_3$Rs, the generation of an array of physiological and pharmacological tools has provided the clearest delineation of the mechanisms by which these receptors are involved in chronic pain. Specific $P2X_3$R antibodies, $P2X_3$- and $P2X_{2/3}$R-deleted transgenic mice, successful *in vivo* $P2X_3$R antisense oligonucleotide strategies and, importantly, the selective and potent $P2X_3$R/$P2X_{2/3}$R antagonist, A-317491 (Jarvis *et al*., 2002), have provided a rather detailed picture of where and how this P2XR subtype

Correspondence: Professor A Surprenant, Institute of Molecular Physiology, University of Sheffield, Alfred Denny Building, Western Bank, Sheffield S10 2TN, UK.
E-mail: a.surprenant@sheffield.ac.uk
Received 23 June 2006; revised 22 August 2006; accepted 5 September 2006; published online 9 October 2006

functions (North, 2002; Jarvis, 2003; Kennedy *et al*., 2003; McGaraughty *et al*., 2003; North 2004; Chen *et al*., 2005; Liu and Salter, 2005; Tsuda *et al*., 2005).

In contrast to the wealth of data concerning neuronal P2X$_3$-containing receptors and pain mechanisms, similar data concerning P2X$_4$Rs and P2X$_7$Rs lag behind, primarily owing to a lack of selective receptor antagonists (Baraldi *et al*., 2004). P2X$_4$Rs are the most ubiquitously and highly expressed of all P2XRs; they are found not only throughout the peripheral and central nervous system but also in non-neuronal cells, particularly epithelial and immune cells (North, 2002; Burnstock and Knight, 2004). P2X$_7$Rs show a more localized expression pattern; they are clearly observed in many immune cells and epithelia but not generally in neurones (Burnstock and Knight, 2004; Sim *et al*., 2004; Anderson and Nedergaard, 2006). Importantly, these two receptors are found in the same populations of immune cells and are both upregulated in macrophage and microglia in response to inflammatory stimuli such as endotoxins and also by peripheral nerve injury (La Sala *et al*., 2003; Burnstock and Knight, 2004; Inoue *et al*., 2004; Tsuda *et al*., 2005). Moreover, they have both been implicated in neuropathic hypersensitivity following peripheral nerve injury (Inoue *et al*., 2004; Chessell *et al*., 2005; Schwab *et al*., 2005). This close physical and potential functional association between P2X$_4$Rs and P2X$_7$Rs in activated macrophage and microglia highlights the particular need for compounds that can clearly differentiate P2X$_4$ from P2X$_7$R activation.

The High-Throughput-Screening and Hit-to-Lead groups at AstraZeneca have briefly described two different series of compounds that are potent inhibitors of P2X$_7$R-mediated ethidium uptake in the human tamm-horsefall protein-1 (THP-1) monocyte cell line, a series of cyclic imides (Alcaraz *et al*., 2003) and a series of adamantane amides (Baxter *et al*., 2003). However, these compounds have not been investigated for their selectivity at P2X$_7$R relative to other P2X and P2Y receptors (P2YRs), nor have species specificity and other assays been examined. We have therefore undertaken a series of experiments on one of the cyclic imides, AZ11645373 (Alcaraz *et al*., 2003; compound 8h), to characterize its actions at P2X$_7$Rs using a variety of cell-based assays and to examine its selectivity at other P2XRs. We find AZ11645373 to be a highly potent antagonist at human P2X$_7$Rs (hP2X$_7$Rs) with half-maximal antagonist concentration ($IC_{50}$) values ranging from 5 to 90 nM depending on the cellular assay. It is only weakly inhibitory at rat P2X$_7$Rs (rP2X$_7$Rs) ($IC_{50} > 10\,\mu$M), and is without effect at other P2XRs at concentrations up to 10 $\mu$M.

## Methods

*Cells*

Human embryonic kidney cell line (HEK293) cells stably expressing human P2X$_1$, P2X$_3$, P2X$_4$, P2X$_7$, rat P2X$_2$, P2X$_{2/3}$, P2X$_4$, P2X$_7$, or transiently expressing a full-length human P2X$_5$R, were used as described in detail previously (Jiang *et al*., 2000). Cells were maintained in DMEM:F12 medium containing 10% foetal calf serum (FCS) and 2 mM L-glutamine at 37°C in a humidified 5% $CO_2$ incubator. Human THP-1 monocytes were maintained in Roswell Park Memorial Institute 1640 media containing 10% FCS and 2 mM L-glutamine.

*Electrophysiology and video imaging*

Whole-cell patch-clamp recordings were performed at room temperature using an EPC9 amplifier and Pulse acquisition software (HEKA, Lambrecht, Germany). Agonists and antagonists were delivered using the RSC fast-flow system (Bio-Logic Science Instruments, Grenoble, France), antagonists were also present in the superfusion solution 4–12 min before application of agonist from flow tubes containing both agonist and antagonist. Unless otherwise stated, internal/external solutions were as follows (mM): NaCl 145, 4-(2-hydroxyethyl)-1-piperazineethyl-sulphonic acid (HEPES) 10, ethylene glycol-bis(â-aminoethyl ether)-*N*,*N*,*N*′,*N*′,-tetraacetic acid (EGTA) 10/NaCl 145, KCl 2, $CaCl_2$ 2, $MgCl_2$ 1, HEPES 10, glucose 13; pH 7.3, osmolarity 300–310 mosmol l$^{-1}$. Low-divalent external solution contained zero $MgCl_2$ and 0.2 mM $CaCl_2$. Membrane potential was clamped at −60 mV in all experiments other than those where ramp protocol (−120 to 60 mV over 1 s) was used to examine voltage dependence. YO-PRO1 fluorescence was measured using the same setup and protocols. Cells were imaged under ×10 objective on a Zeiss Axiovert 100 microscope, images collected (1 frame s$^{-1}$) with a Hamamatsu 1394 ORCA-285 CCD camera using Simple PCI software (Digital Imaging Systems, Brighton, UK). YO-PRO1 (3 $\mu$M) was present in all solutions, fluorescence intensity from 25 to 100 cells in field of view were averaged.

*Fluo4-AM calcium measurements*

Human embryonic kidney (HEK) cells were loaded with Fluo4-AM (3 $\mu$M) for 30 min at 37°C in loading buffer (mM: NaCl 136, KCl 1.8, $KH_2PO_4$ 1.2, $MgSO_4$ 1.2, $NaHCO_3$ 5, $CaCl_2$ 2, glucose 6, HEPES 20 and EGTA 5). Cells were washed once and resuspended in loading buffer without EGTA. Cells ($10^6$ in 1 ml) were placed in a cuvette for $Ca^{2+}$ measurements using the Cairn Integra fluorimeter (Cairn Research, Kent, UK). Cumulative agonist concentration–response curves were obtained and results normalized to maximum fluorescence induced by digitonin (20 $\mu$M) applied at the end of the experiment. Digitonin-induced fluorescence varied by <10% in a single set of experiments (six cuvettes/experiment; e.g. Figure 3a).

*Interleukin-1β release*

THP-1 monocytes were plated in 24-well plates at $6 \times 10^5$ cells ml$^{-1}$ in culture medium; phorbol myristate acetate (0.5 $\mu$M) was added for 30 min and then the medium was replaced with serum-free medium containing 100 ng ml$^{-1}$ lipopolysaccharide (LPS) with or without AZ11645373 for 4 h. Medium was then removed and replaced with 200 $\mu$l medium containing ATP (3 mM) with or without AZ11645373 for 30 min. Supernatants were collected and assayed for interleukin-1$\beta$ (IL-1$\beta$) by enzyme-linked immunosorbent assay (ELISA) using plates coated with anti-human IL-1$\beta$ (2 $\mu$g ml$^{-1}$,

Perbio Science Ltd, Cramlington, UK). IL-1$\beta$ was detected with polyclonal biotinylated anti-human IL-1$\beta$ (0.5 $\mu$g ml$^{-1}$). This assay recognizes both pro-IL-1$\beta$ and processed IL-1$\beta$. Assays were performed in triplicate and results from individual experiments averaged.

*Data analysis*

Concentration–response (membrane currents or Fluo4 fluorescence) curves were obtained in the absence or presence of increasing concentrations of AZ11645373. For each assay, preliminary experiments were carried out to determine time to equilibrium response for each antagonist concentration; these ranged from 2 to 4 min in the Fluo4 fluorimeter assay to 10–12 min in the YO-PRO1 assay. All data presented in this study were obtained at time points could be considered to have reached equilibrium conditions. Numerical estimates of agonist effector concentration for half-maximum response ($EC_{50}$) values were made by least squares curve fitting as described previously (Jiang *et al*., 2000), using the function $I/I_{max} = [A]^n/(EC_{50}^n + [A]^n)$, where $I$ is the current, or Fluo4 fluorescence, as a fraction of the maximum ($I_{max}$) and [A] is concentration of ATP or 2′-3′-*O*-(4-benzoylbenzoyl) adenosine 5′-triphosphate (BzATP). Figures show this function fitted to the mean of all experiments, points are mean ± s.e.m. Inhibition curves were constructed by plotting the response ($I$, (current amplitude), fluorescence intensity or IL-1$\beta$ released) as a fraction of its response in the absence of AZ11645373 ($I_0$), as a function of the concentration of AZ11645373 ($B$). $IC_{50}$ values were calculated by least-squares fitting of mean values to $I/I_0 = 1/(1 + (IC_{50}/B)^n)$. The dissociation equilibrium constant ($K_B$) for AZ11645373 was estimated on the assumption that the antagonism was insurmountable by fitting agonist concentrations ($A$) and antagonist concentrations ($B$) to $I/I_0 = 1/((1 + (EC_{50}/A))(1 + (B/K_B)))$ (Kenakin, 1990). All curve fits were generated using Kaleidagraph (Synergy Software, Reading, PA, USA). Tests of significance were by Student's $t$-test, analysis of variance and Tukey–Kramer multiple comparisons test using Instat 3 software (GraphPad Inc., www.graphpad.com).

*Reagents*

Culture media, sera and other cell culture reagents were obtained from Life Technologies (Paisley, UK), YO-PRO1 iodide and Fluo4-AM from Molecular Probes (Invitrogen, Paisley, UK), ATP and BzATP from Sigma-Aldrich (Poole, UK). Synthesis of AZ11645373 (Figure 1) was as described previously (Alcaraz *et al*., 2003). Because earlier studies had revealed that this compound could be subjected to slow hydrolysis by nucleotides (Alcaraz *et al*., 2003), AZ11645373 was continuously superfused during electrophysiological and fluorescence imaging experiments and was added to agonist-containing solutions only immediately before application. However, it is unlikely that compound breakdown was a significant factor in these experiments because we obtained similar levels of inhibition even when AZ11645373 was in contact with ATP or BzATP for up to 2 h.

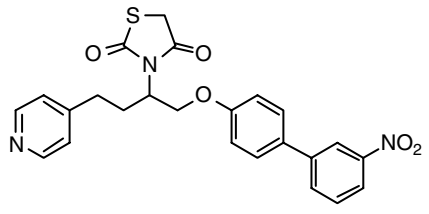


**Figure 1** Chemical structure of AZ11645373.

## Results

*Inhibition of P2X$_7$R-evoked membrane currents*

ATP and BzATP concentration–current curves were generated during whole-cell recordings from HEK cells expressing either human or rP2X$_7$Rs in the absence and presence of increasing concentrations of AZ11645373 (Figure 2a and b). These experiments were performed in normal extracellular solution as well as in low-divalent-containing extracellular solution, in view of previous studies on P2X$_7$Rs which have found that antagonist potencies of the non-selective P2XR

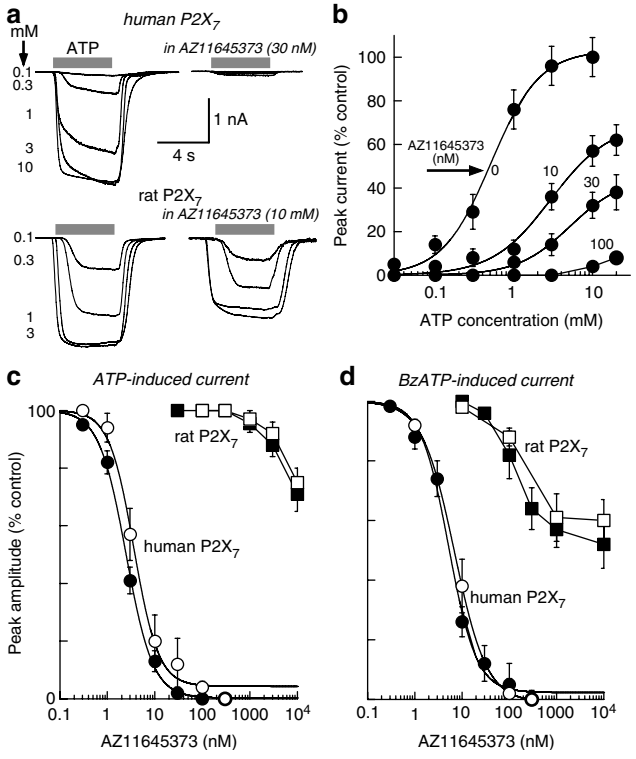


**Figure 2** Inhibition of membrane currents activated by P2X$_7$Rs expressed in HEK cells by AZ11645373. (**a**) Superimposed traces of currents recorded from human or rP2X$_7$-expressing cells in the absence and presence of AZ11645373 as indicated. Increasing concentrations of ATP were applied for duration indicated by bars; recordings obtained from the same cell in each example. (**b**) Summary of all experiments as illustrated in (**a**) on hP2X$_7$R-expressing cells; $n = 3$–8 separate experiments for each antagonist concentration. (**c**, **d**) AZ11645373 inhibition curves for ATP (**c**) and BzATP (**d**) induced membrane currents in normal external solutions (filled symbols) and in low-divalent solution (open symbols). Approximate $EC_{50}$ concentrations of agonist were used; these were 1 and 0.3 mM ATP for hP2X$_7$R in normal and low-divalent solutions, respectively, 0.3 and 0.1 mM ATP for rP2X$_7$R, 0.3 and 0.1 mM BzATP for hP2X$_7$R and 0.03 and 0.01 mM BzATP for rP2X$_7$R. Each point is mean ± s.e.m. from 3 to 9 separate experiments.

antagonists, suramin and pyridoxalphosphate-6-azophenyl-2′-4′-disulfonic acid (PPADS), vary significantly depending on the extracellular divalent cation environment (Michel *et al*., 1999). $EC_{50}$ values for ATP and BzATP at the hP2X$_7$R were $1.8\pm0.2$ mM and $210\pm25$ $\mu$M in normal divalent cations and $720\pm22$ and $55\pm6$ $\mu$M in low-divalent cations ($n=6$ for each); these values are similar to those observed in previous studies (Rassendren *et al*., 1997; Michel *et al*., 1999; Jiang *et al*., 2000). AZ11645373 produced similar concentration-dependent inhibition of agonist-evoked currents in either extracellular solution; the inhibition of agonist-evoked currents was non-surmountable at concentrations $\geqslant10$ nM (Figure 2b). Onset of inhibition ranged from approximately 4 min at concentrations $<10$ nM to less than 30 s with concentrations $>1$ $\mu$M. Inhibition of ATP- and BzATP-evoked currents by AZ11645373 was slowly reversible; at concentrations $<1$ $\mu$M currents reversed to $\pm10$% of control values within 15–25 min but full recovery was not observed up to 30 min after washout of higher concentrations of the antagonist. In contrast to the potent inhibition of agonist-evoked currents at the hP2X$_7$R, AZ11645373 (0.01 and 0.1 $\mu$M) produced no significant effect on ATP-evoked concentration–response curves at the rP2X$_7$R in either normal or low-divalent-containing solutions ($n=3$). Higher concentrations (1 and 10 $\mu$M) reduced responses by $<50$% at all agonist concentrations ($n=4$). Because of the apparent non-surmountable nature of AZ11645373 at P2X$_7$R-induced ionic currents, we also carried out AZ11645373 concentration-inhibition experiments using approximately $EC_{50}$ concentrations of ATP and BzATP at human and rP2X$_7$Rs (Figure 2c and d), in order to obtain estimates of antagonist $K_B$ values (Kenakin, 1990, 1993; Jiang *et al*., 2000). Results from these experiments yielded $K_B$ values at hP2X$_7$R of 5 nM when ATP was the agonist and 7 nM when BzATP was the agonist, again with no significant differences observed between normal divalent and low-divalent external solution (Figure 2c and d; Table 1). The inhibition of current by AZ11645373 at hP2X$_7$Rs was voltage independent; similar inhibition was observed at membrane potentials from $-120$ to 60 mV using voltage ramp protocols ($n=4$). We could not obtain $K_B$ estimates at rP2X$_7$R because even the highest concentration of AZ11645373 examined (10 $\mu$M) produced less than 40% inhibition of the ATP-evoked current and less than 55% inhibition of the BzATP-evoked current (Figure 2c and d; Table 1).

**Table 1** Estimated antagonist affinity constants ($K_B$) for AZ11645373 obtained in different assays, using ATP or BzATP as agonist, and in normal or low-divalent containing extracellular solutions

| *Cell type* | *Assay* | $K_B$ *(nM)* | |
|---|---|---|---|
| | | *ATP agonist* | *BzATP agonist* |
| hP2X$_7$-HEK | | | |
| | *Ionic current* | | |
| | Normal | $9\pm4$ (8) | $7\pm4$ (6) |
| | Low divalents | $6\pm4$ (8) | $9\pm5$ (5) |
| | *Ca++ influx* | | |
| | Normal | | $15\pm3$ (7) |
| | *YO-PRO1 uptake* | | |
| | Normal | $18\pm4$ (6) | $20\pm4$ (5) |
| | Low divalents | $15\pm3$ (4) | $17\pm3$ (5) |
| THP-1 monocyte | | | |
| | *YO-PRO1 uptake* | | |
| | Normal | $17\pm3$ (4) | $21\pm4$ (3) |
| | IL-1$\beta$ release | $92\pm9$ (8)** | |
| RP2X$_7$-HEK | | | |
| | *Ionic current* | | |
| | Normal | $>10\,000$ | $>10\,000$ |
| | Low divalents | $>10\,000$ | $>10\,000$ |
| | *YO-PRO1 uptake* | | |
| | Normal | $>10\,000$ | |
| | Low divalents | $>10\,000$ | $>10\,000$ |

Abbreviations: ATP, adenosine 5′-triphosphate; BzATP, 2′-3′-*O*-(4-benzoyl-benzoyl) adenosine 5′-triphosphate; HEK, human embryonic kidney; THP-1, tamm-horsefall protein-1.
There were no significant differences in any values ($P>0.05$) with the exception of IL-1$\beta$ release, which was significantly different from values obtained in all other conditions ($P<0.01$ indicated by asterisks). Numbers in parentheses are numbers of experiments.

*Inhibition of P2X$_7$R-mediated cytosolic calcium increases*

HEK cells express several G-protein-coupled P2YRs whose activation by ATP, adenosine diphosphate and/or uracil triphosphate (UTP) results in increases in cytosolic calcium, whereas BzATP is generally ineffective at concentrations $<100$ $\mu$M (Schachter *et al*., 1997; Wilson *et al*., 2002; Fischer *et al*., 2005). We initially examined the actions of AZ11645373 (0.1 and 10 $\mu$M) on ATP (30 $\mu$M)- and UTP (30 $\mu$M)-evoked calcium transients using Fluo4-AM in untransfected HEK cells and found no significant inhibition of these responses (Figure 3d). These calcium responses showed typical P2YR-mediated desensitizing kinetics in the continued presence of ATP or UTP (Figure 3d). BzATP, at concentrations $\leqslant100$ $\mu$M, did not evoke calcium transients in untransfected HEK cells, whereas at concentrations $\geqslant300$ $\mu$M typical P2YR-like desensitizing calcium transients were evoked which were insensitive to inhibition by AZ11645373 (10 $\mu$M, $n=5$). In contrast, continuous application of BzATP ($>100$ $\mu$M) in P2X$_7$R-expressing HEK cells produced only sustained calcium responses (Figure 3a). Moreover, AZ11645373 produced a concentration-dependent inhibition of BzATP-mediated calcium transients with complete inhibition observed at concentrations between 100 and 300 nM based on concentration–inhibition curves (Figure 3a–c). These results allow us to conclude firstly, that ATP-, UTP- and BzATP-sensitive P2YRs expressed in the untransfected HEK cells used in these experiments are not inhibited by AZ11645373 and secondly, that our HEK cells stably expressing hP2X$_7$Rs do not possess BzATP-sensitive P2YRs. Therefore, we can be fairly certain that the inhibition profile of AZ11645373 in this calcium mobilization assay results solely from inhibition of P2X$_7$Rs. The $K_B$ value determined from AZ11645373 inhibition curves using BzATP in this cellular assay was 15 nM (Table 1).

*Inhibition of P2X$_7$R-induced YO-PRO1 uptake*

Uptake of membrane-impermeant fluorescent dyes, such as ethidium and YO-PRO1, is a hallmark of early downstream signalling by P2X$_7$Rs and was the means for drug discovery of the cyclic imides by high-throughput screening using

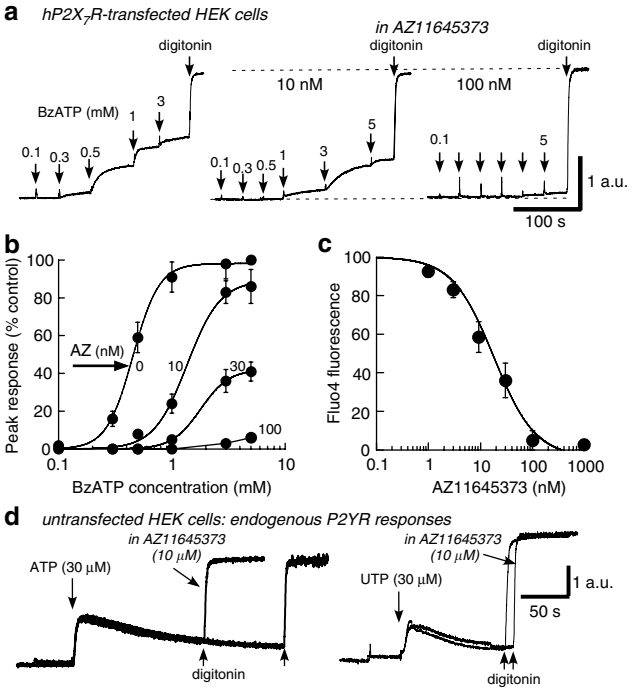


**Figure 3** Inhibition of calcium mobilization at hP2X$_7$R-expressing HEK cells by AZ11645373 and lack of effect at endogenous P2YRs in non-P2X$_7$R-expressing cells. (**a**) Representative traces of Fluo4-AM fluorescence in response to cumulative additions of BzATP (as indicated at arrows) in the absence or presence of AZ11645373 as indicated. Digitonin (20 $\mu$M final volume) added before completion of experiment to determine maximum cytosolic calcium signal; all data were normalized to this value. (**b**) Averaged data obtained from all experiments as illustrated in (**a**); $n=4$ for all points. (**c**) AZ11645373 inhibition curves from experiments in which approximate $EC_{50}$ concentration of BzATP (0.3 mM) were used; $n=6$ for each point. (**d**) Fluo4-AM fluorescence in response to ATP or UTP (30 $\mu$M) in untransfected HEK cells; superimposed traces are in the absence or presence of AZ11645373 (10 $\mu$M) as indicated. Similar lack of effect of AZ11645373 was recorded in five separate experiments.

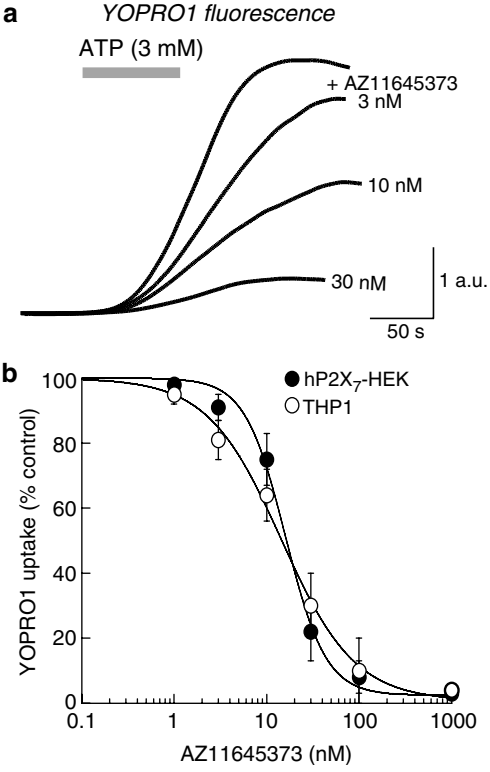


**Figure 4** Inhibition of ATP-induced YO-PRO1 uptake by AZ11645373 in hP2X$_7$R-expressing HEK cells and THP-1 human monocytes. (**a**) Representative traces of YO-PRO1 fluorescence in response to ATP applied for duration indicated by bar in the absence or presence of AZ11645373 as indicated; superimposed traces are averaged traces from 25 to 45 cells in field of view from separate coverslips. (**b**) Summary of all experiments as illustrated in (**a**) for hP2X$_7$R-expressing HEK cells (filled symbols; $n=8$) or THP-1 cells (open symbols; $n=4$).

THP-1 monocytes expressing endogenous P2X$_7$Rs (Alcaraz *et al*., 2003). In accord with many previous studies on ectopically expressed P2X$_7$Rs (Rassendren *et al*., 1997; Michel *et al*., 1999; see North, 2002), ATP- and BzATP-evoked YO-PRO1 uptake in P2X$_7$R-expressing (Figure 4a), but not in untransfected or hP2X$_4$R-expressing HEK cells (data not shown). The maximum YO-PRO1 fluorescence was 10- to 15-fold greater in cells expressing rP2X$_7$R than in cells expressing hP2X$_7$R, even though maximum membrane current amplitudes were similar; these findings are also similar to those observed in previous studies (Rassendren *et al*., 1997; Hibell *et al*., 2001). AZ11645373 inhibited ATP- or BzATP-evoked YO-PRO1 fluorescence in HEK cells stably expressing hP2X$_7$R, but not rP2X$_7$R-expressing cells with a $K_B$ value that was not significantly different from those obtained in experiments measuring membrane current or calcium mobilization (Figure 4a and b; Table 1). YO-PRO1 fluorescence was also measured from human THP-1 cells endogenously expressing P2X$_7$R under identical protocols; the inhibition by AZ11645373 and the calculated $K_B$ value was not significantly different from that obtained from HEK cells ectopically expressing hP2X$_7$R (Figure 4b, Table 1).

*Inhibition of P2X$_7$R-mediated IL-1β release*

IL-1$\beta$ release from LPS-stimulated THP-1 monocytes in response to ATP is now well established as resulting from activation of P2X$_7$Rs (Labasi *et al*., 2002; Dinarello, 2005). Therefore, we examined the actions of AZ11645373 in this therapeutically significant cellular assay. AZ11645373 alone (1 $\mu$M) had no significant effect on basal levels of IL-1$\beta$ in the medium of LPS-treated cells (Figure 5a), but produced a concentration-dependent inhibition of ATP-mediated release of IL-1$\beta$ (Figure 5a and b) with a calculated $K_B$ value of 92 nM (Table 1).

*Lack of effect at other P2XRs*

Finally, we examined the selectivity of AZ11645373 at other P2XRs, paying particular attention to hP2X$_4$R in view of its intimate association with P2X$_7$Rs (see Introduction). Complete ATP concentration–membrane current curves were generated in the absence and presence of AZ11645373 in HEK cells expressing hP2X$_4$Rs; no significant differences were observed at concentrations up to 10 $\mu$M (Figure 6a and b). Lower concentrations of AZ11645373 (0.1 and 1 $\mu$M) were also without effect ($n=2$). For the other P2XRs, $EC_{50}$ concentrations of agonist were used; AZ11645373 (10 $\mu$M) had no significant effect on ionic currents recorded in

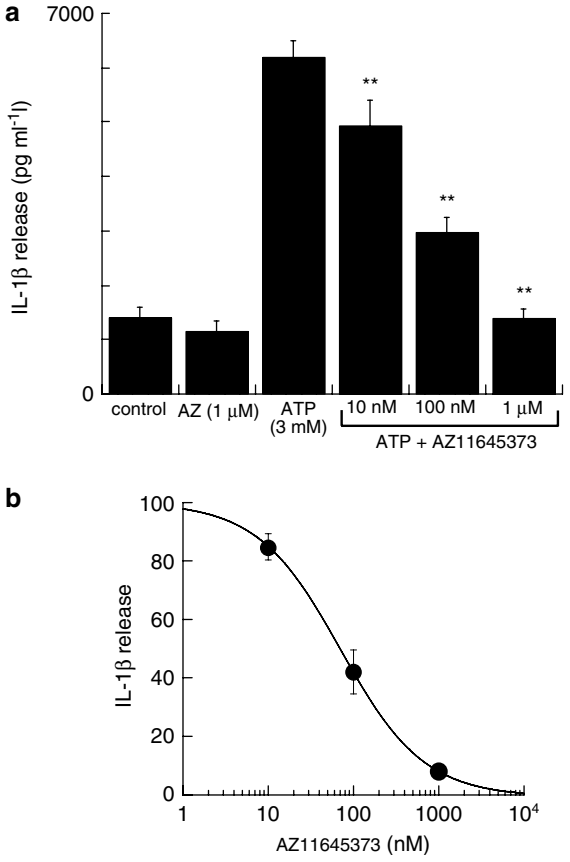


**Figure 5** AZ11645373 inhibition of ATP-induced IL-1$\beta$ release from LPS-stimulated THP-1 monocytes. (**a**) IL-1$\beta$ measured by ELISA from supernatants collected 30 min after ATP in the absence or presence of 10, 100 or 1000 nM AZ11645373 as indicated; control and AZ11645373 alone are in the absence of ATP. Histogram shows mean$\pm$s.e.m. from triplicate wells; asterisks indicate significantly different from ATP alone and release in the presence of ATP$+1$ $\mu$M AZ11645373 was not significantly different from control value. (**b**) Averaged results from all experiments illustrated in (**a**) where IL-1$\beta$ release is plotted as % of control (ATP in the absence of antagonist); $n=4$ for each point.

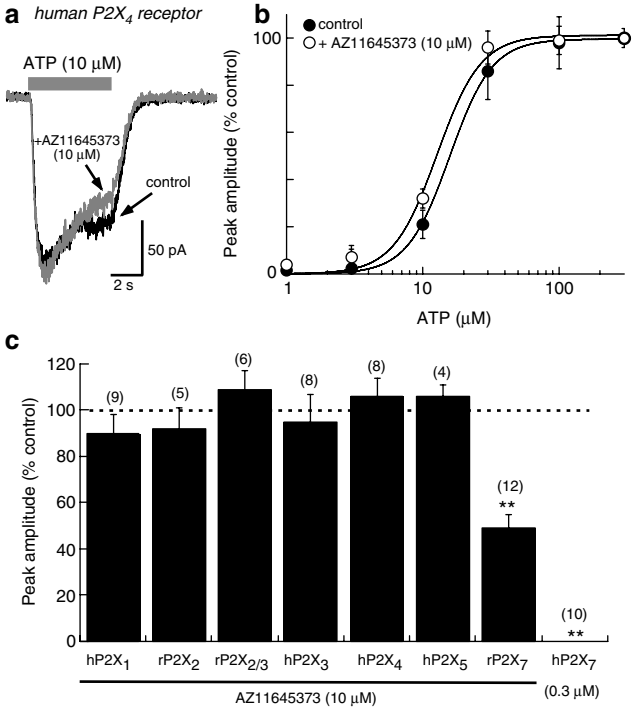


**Figure 6** Lack of effect of AZ11645373 at other P2XRs. (**a**) Superimposed traces of ATP-evoked currents from hP2X$_4$R-expressing HEK cell in the absence and presence of 10 $\mu$M AZ11645373. (**b**) ATP concentration–response curves for membrane currents at hP2X$_4$R-expressing cells in the absence and presence of 10 $\mu$M AZ11645373 as indicated; $n=4$ for each point and there were no significant differences at any agonist concentration. (**c**) Histogram summarizing results obtained at other P2XRs. Data are expressed as % control amplitude using approximate EC$_{50}$ agonist concentrations for each receptor; these were 1 $\mu$M ATP for hP2X$_1$R, 20 $\mu$M ATP for rP2X$_2$R, 3 $\mu$M $\alpha\beta$me-ATP for rP2X$_{2/3}$R, 30 $\mu$M for hP2X$_4$R and 10 $\mu$M ATP for hP2X$_5$R. Also shown are results for rP2X$_7$R using 1 mM ATP and for hP2X$_7$R using 3 mM ATP and in the presence of lower concentration of AZ11645373 as indicated. Asterisks indicate significant difference from control value.

response to activation of any of these P2XRs (Figure 6c). This concentration of AZ11645373 also had no effect on membrane currents when applied in the absence of agonist.

## Discussion

This study has provided a detailed pharmacological characterization of a newly identified P2X$_7$R antagonist, AZ11645373, using a repertoire of cellular assays. AZ11645373 was highly effective at inhibiting ATP- and BzATP-mediated responses in all our assays on hP2X$_7$Rs, with IC$_{50}$/$K_B$ values ranging from 5 to 90 nM depending on the specific assay (Table 1). It was also highly selective for hP2X$_7$R over rP2X$_7$R where even 500-fold higher concentrations (10 $\mu$M) inhibited rP2X$_7$R-mediated membrane currents by only 40–50%. It was completely without effect at all other P2XR subtypes and was equally ineffective at endogenous P2YRs present in HEK cells. Thus, this compound becomes one of the most significant new additions to the currently poor arsenal of P2X$_7$R-specific ligands.

The inhibition of hP2X$_7$R responses by AZ11645373 exhibits some features common to, as well as prominent differences from, other known inhibitors of this receptor. Common features are the generally insurmountable profile of the inhibition and the striking species-specific inhibition; significant differences are the relatively small variability in IC$_{50}$ or $K_B$ values among the assays examined, the similar inhibition observed using either normal or low-divalent-containing external solutions, and the complete lack of effect on other P2XRs.

Compounds that are known to inhibit at least some P2X$_7$-mediated responses are suramin, PPADS, oxidized ATP, KN-62, calmidizolium and Brilliant Blue G; these all act in a non-competitive manner at ATP- or BzATP-evoked membrane currents and/or ethidium/YO-PRO1 uptake (North, 2002; Baraldi *et al*., 2004). These compounds also exhibit significant species differences; for example, KN-62 inhibits membrane currents, calcium mobilization and dye uptake induced by activation of hP2X$_7$Rs with an IC$_{50}$ value of approximately 10 nM but has no significant action at

rP2X$_7$Rs at micromolar concentrations (Humphreys *et al*., 1998). Conversely, Brilliant Blue G is 30- to 50-fold more potent at inhibiting rP2X$_7$Rs than hP2X$_7$Rs, with IC$_{50}$ values of approximately 10 and 300 nM, respectively (Jiang *et al*., 2000). These types of differences are to be expected in view of the relatively low sequence identity/conservation between rP2X$_7$Rs/hP2X$_7$Rs (80% in the ectodomain); this is significantly less than at other P2XRs where identity/conservation is generally 90–99% when comparing rat versus human orthologues (North, 2002). Most importantly, all of these compounds exert effects at several other membrane proteins including other P2XRs. Suramin, PPADS and oxidized ATP inhibit most other P2XRs and/or P2YRs, as well as other ligand-gated ion channels, ectonucleotidases and numerous intracellular enzymes, and are well accepted as being of only limited value for differentiating physiological functions attributable to specific P2XR or P2YR subtypes (North, 2002; Baraldi *et al*., 2004). Similarly, calmidazolium, as well as KN-62 and several of its analogues, are better known for their inhibition of calmodulin and calcium-calmodulin kinase II (Braun and Schulman, 1995). Brilliant Blue G has proved the most useful P2X$_7$R antagonist to date owing to its low nanomolar affinity at rP2X$_7$R, but it is only 10-fold selective for hP2X$_7$R over hP2X$_4$R and inhibits rP2X$_2$R and some P2YRs in the low micromolar range. (Soltoff *et al*., 1989; King *et al*., 1996; Jiang *et al*., 2000). The present study has shown that AZ11645373 had no significant agonist or antagonist action at any other P2XR at concentrations up to 10–20 $\mu$M and did not alter endogenous P2Y-mediated calcium transients at these concentrations. Based on previous studies with Brilliant Blue G (Jiang *et al*., 2000), and the present study with AZ11645373, we can conclude that Brilliant Blue G currently remains the more selective P2X$_7$R antagonist in physiological and pharmacological studies using rats or cells expressing rP2X$_7$Rs, but AZ11645373 is now clearly the P2X$_7$R antagonist of choice for studies using human cells.

The affinity of AZ11645373 at hP2X$_7$Rs was not significantly different in experiments using either ATP or BzATP, or in experiments using normal or low-divalent cations. These findings are in contrast to the inhibition by other P2X$_7$R inhibitors (suramin, PPADS, KN-62, oxidized ATP and Brilliant Blue G) where IC$_{50}$ values can differ by 10- to 20-fold depending on agonist and/or extracellular environment (Chessell *et al*., 1998; Michel *et al*., 1999; Hibell *et al*., 2001). Such differences have complicated comparisons of these antagonists among various studies in the past. AZ11645373 will therefore be of much practical value given that many investigations of P2X$_7$R function in isolated cells use different agonists and low-divalent-containing solutions.

We compared the inhibition of hP2X$_7$Rs by AZ11645373 in all of the commonly used cellular assays; that is, ionic currents, calcium flux, dye uptake and IL-1$\beta$ release from LPS-stimulated monocyte/macrophage (Perregaux and Gabel, 1994; Di Virgilio *et al*., 1996; North, 2002). There were no significant differences in IC$_{50}$/$K_B$ values obtained from patch-clamp, Fluo4 or YO-PRO fluorescence assays (Table 1), whereas the IC$_{50}$ value for ATP-evoked IL-1$\beta$ release was about 10-fold higher. It is unlikely this represents a real difference in affinity of AZ11645373 for endogenous P2X$_7$Rs present in THP-1 monocytes versus ectopically expressed hP2X$_7$Rs because the $K_B$/IC$_{50}$ values for inhibition of ATP-evoked YO-PRO1 uptake were similar in the THP-1 cells and the hP2X$_7$-expressing HEK cells (Figure 4; Table 1). It is more likely owing to differences in assay conditions and/or the signal cascade measured. The concentration of ATP used in the IL-1$\beta$ release assay was near maximal and so would reduce the apparent effectiveness of a competing antagonist; EC$_{50}$ levels of agonist were used for the patch-clamp and Fluo4 studies. Ionic current and calcium influx are immediate upstream signals activated in milliseconds, YO-PRO1 dye uptake is also an early event, occurring in seconds. In contrast, IL-1$\beta$ release is a relatively late downstream event requiring a cascade of proteolytic processes and release mechanisms (Dinarello, 2005). Additionally, it is not yet technically possible to follow IL-1$\beta$ release in real time from single cells, requiring this assay to rely on ELISA measurements made from superfusate collected from populations of cells after longer term (30–60 min) exposure to agonist. Irrespective of these differences, drug receptor theory argues that the same affinity constant should be obtained assuming agonist/antagonist equilibrium conditions (Kenakin, 1990, 1993). It may be that the duration of agonist application (5–20 s for membrane currents, 2–5 min for Fluo4 and YO-PRO1 fluorescence assays) is insufficient for adequate equilibrium conditions, thus yielding an underestimated $K_B$ value from data obtained by electrophysiological or fluorescence measurements. Results from an earlier study measuring ethidium uptake from THP-1 cells after 90 min incubation with BzATP gave a $K_B$ estimate of 20 nM for AZ11645373 (Alcaraz *et al*., 2003), which is very similar to that obtained in the present study, but the profile was more competitive in nature that observed in the present study and this is consistent with equilibrium conditions influencing affinity estimates. In spite of the range in values obtained from electrophysiological and fluorescence assays (4–30 nM), mean values were not significantly different among the assays (Table 1). In any event, we observed significant inhibition of ATP-induced IL-1$\beta$ release at 10 nM AZ11645373 and complete block at 1 $\mu$M thereby validating its effectiveness in inhibiting hP2X$_7$R-mediated IL-1$\beta$ release.

Although much remains to be learned about the mechanisms by which P2X$_7$Rs couple to release of the proinflammatory cytokine, IL-1$\beta$, and their role in inflammatory processes, it has been apparent for more than a decade that they represent a potentially important therapeutic target for inflammatory diseases (Di Virgilio *et al*., 1996). The ability of AZ11645373 to unequivocally differentiate responses due to the activation of hP2X$_7$Rs from those due to other P2XRs, particularly hP2X$_4$R, makes it of particular significance for *in vitro* functional studies in human cells and cell lines. This will be especially revealing for studies in immune cells where these receptors colocalize and where they both may play a role in inflammatory processes.

## Acknowledgements

We thank E Martin and W Ma for cell biology support.

## Conflict of interest

The authors state no conflict of interest.

## References

Alcaraz L, Baxter A, Bent J, Bowers K, Braddock M, Cladingboel D *et al.* (2003). Novel P2X$_7$ receptor antagonists. *Bioorg Med Chem Lett* **13**: 4043–4046.

Anderson CM, Nedergaard M (2006). Emerging challenges of assigning P2X7 receptor function and immunoreactivity in neurons. *Trends Neurosci* **29**: 257–262.

Baraldi PG, Di Virgilio F, Romagnoli R (2004). Agonists and antagonists acting at P2X7 receptor. *Curr Top Med Chem* **4**: 1707–1717.

Baxter A, Bent J, Bowers K, Braddock M, Brough S, Fagura M *et al.* (2003). Hit-to-Lead studies: the discovery of potent adamantane amide P2X$_7$ receptor antagonists. *Bioorg Med Chem Lett* **13**: 4047–4050.

Braun AP, Schulman H (1995). The multifunctional calcium/calmodulin-dependent protein kinase: from form to function. *Annu Rev Physiol* **57**: 417–445.

Burnstock G, Knight GE (2004). Cellular distribution and functions of P2 receptor subtypes in different systems. *Int Rev Cytol* **240**: 31–304.

Chen Y, Li G-W, Wang C, Gu Y, Huang L-Y (2005). Mechanisms underlying enhanced P2X receptor-mediated responses in neuropathic pain state. *Pain* **119**: 38–48.

Chessell IP, Hatcher JP, Bountra C, Michel AD, Hughes JP, Green P *et al.* (2005). Disruption of the P2X7 purinoceptor gene abolishes chronic inflammatory and neuropathic pain. *Pain* **114**: 386–396.

Chessell IP, Michel AD, Humphrey PPA (1998). Effects of antagonists at the human recombinant P2X$_7$ receptor. *Br J Pharmacol* **124**: 1314–1320.

Dinarello CA (2005). Blocking IL-1 in systemic inflammation. *J Exp Med* **201**: 1355–1359.

Di Virgilio F, Ferrari D, Falzoni S, Chiozzi P, Munerati M, Steinberg TH *et al.* (1996). P2 purinoceptors in the immune system. *Ciba Found Symp. 198 P2 Purinoceptors: Localization, Function and Transduction Mechanisms* **198**: 290–305.

Fischer W, Franke H, Groger-Arndt H, Illes P (2005). Evidence for the existence of P2Y$_{1,2,4}$ receptor subtypes in HEK-293 cells: reactivation of P2Y$_1$ receptors after repetitive agonist application. *Naunyn-Schmiedebergs Arch Pharmacol* **371**: 466–472.

Hibell AD, Thompson KM, Xing M, Humphrey PPA, Michel AD (2001). Complexities of measuring antagonist potency at P2X$_7$ receptor orthologs. *J Pharmacol Exp Ther* **296**: 947–957.

Humphreys BD, Virginio C, Surprenant A, Rice J, Dubyak GR (1998). Isoquinolines as antagonists of the P2X$_7$ nucleotide receptor: high selectivity for the human versus rat receptor homologues. *Mol Pharmacol* **54**: 22–32.

Inoue K, Tsuda M, Koizumi S (2004). ATP- and adenosin-mediated signaling in the central nervous system: chronic pain and microglia: involvement of the ATP receptor P2X4. *J Pharmacol Sci* **94**: 112–114.

Jarvis MF (2003). Contributions of P2X$_3$ homomeric and heteromeric channels to acute and chronic pain. *Expert Opin Ther Targets* **7**: 513–522.

Jarvis MF, Burgard EC, Mcgaraughty S, Honore P, Lynch K, Brennan TJ *et al.* (2002). A-317491, a novel potent and selective non-nucleotide antagonist of P2X$_3$ and P2X$_{2/3}$ receptors, reduces chronic inflammatory and neuropathic pain in the rat. *Proc Natl Acad Sci USA* **99**: 17179–17184.

Jiang L-H, Mackenzie AB, North RA, Surprenant A (2000). Brilliant Blue G selectively blocks ATP-gated P2X$_7$ receptors. *Mol Pharmacol* **58**: 82–88.

Kenakin T (1990). Drugs and receptors. An overview of the current state of knowledge. *Drugs* **40**: 666–687.

Kenakin T (1993). *Pharmacological Analysis of Drug-Receptor Interaction* 2nd edn. Raven Press, New York.

Kennedy C, Assis TS, Currie AJ, Rowan EG (2003). Crossing the pain barrier: P2 receptors as targets for novel analgesics. *J Physiol* **553**: 683–694.

King BF, Dacquet C, Ziganshin AU, Weetman DF, Burnstock G, Vanhoutte PM *et al.* (1996). Potentiation by 2,2′ pyridylisatogen tosylate of ATP-responses at a recombinant P2Y1 purinoceptor. *Br J Pharmacol* **117**: 1111–1118.

Labasi JM, Petrushova N, Donovan C, Mccurdy S, Lira P, Payette MM *et al.* (2002). Absence of the P2X$_7$ receptor alters leukocyte function and attenuates an inflammatory response. *J Immunol* **168**: 6436–6445.

La Sala A, Ferrari D, Di Virgilio F, Idzko M, Norgauer J, Girolomoni G (2003). Alerting and tuning the immune response by extracellular nucleotides. *J Leukocyte Biol* **73**: 339–343.

Liu XJ, Salter MW (2005). Purines and pain mechanisms: recent developments. *Curr Opin Investig Drugs* **6**: 65–75.

Mcgaraughty S, Wismer CT, Zhu CZ, Mikusa J, Honore P, Chu KL *et al.* (2003). Effects of A-317491, a novel and selective P2X$_3$/P2X$_{2/3}$ receptor antagonist, on neuropathic, inflammatory and chemogenic nociception following intrathecal and intraplantar administration. *Br J Pharmacol* **140**: 1381–1388.

Michel AD, Chessell IP, Humphrey PPA (1999). Ionic effects on human recombinant P2X$_7$ receptor function. *Naunyn Schmiedebergs Arch Pharmacol* **359**: 102–109.

North RA (2002). Molecular physiology of P2X receptors. *Physiol Rev* **82**: 1013–1067.

North RA (2004). P2X$_3$ receptors and peripheral pain mechanisms. *J Physiol* **554**: 301–308.

Perregaux D, Gabel CA (1994). Interleukin-1 beta maturation and release in response to ATP and nigericin. Evidence that potassium depletion mediated by these agents is a necessary and common feature of their activity. *J Biol Chem* **269**: 15195–15203.

Rassendren F, Buell GN, Virginio C, Collo G, North RA, Surprenant A (1997). The permeabilizing ATP receptor, P2X$_7$: cloning and expression of a human cDNA. *J Biol Chem* **272**: 5482–5486.

Schachter B, Sromek SM, Nicholas RA, Harden TK (1997). HEK293 human embryonic kidney cells endogenously express the P2Y$_1$ and P2Y$_2$ receptors. *Neuropharmacology* **36**: 1181–1187.

Schwab JM, Guo L, Schluesener HJ (2005). Spinal cord injury induces early and persistent lesional P2X$_4$ receptor expression. *J Neuroimmunol* **163**: 185–189.

Sim JA, Young MT, Sung H-Y, North RA, Surprenant A (2004). Reanalysis of P2X$_7$ receptor expression in rodent brain. *J Neurosci* **24**: 6307–6314.

Soltoff SP, McMillan MK, Talamo BR (1989). Coomassie Brilliant Blue G is a more potent antagonist of P2 purinergic responses than Reactive Blue 2 (Cibacron Blue 3GA) in rat parotid acinar cells. *Biochem Biophys Res Commun* **165**: 1279–1285.

Tsuda M, Inoue K, Salter MW (2005). Neuropathic pain and spinal microglia: a big problem from molecules in 'small' glia. *Trends Neurosci* **28**: 101–107.

Vial C, Roberts JA, Evans RJ (2004). Molecular properties of ATP-gated P2X receptor ion channels. *Trends Pharmacol Sci* **25**: 487–493.

Wilson HL, Wilson SA, Surprenant A, North RA (2002). Epithelial membrane proteins induce membrane blebbing and interact with the P2X$_7$ C-terminus. *J Biol Chem* **277**: 34017–34023.